

## Full Length Article

# Hybrid machine learning-enabled multivariate bridge-specific seismic vulnerability and resilience assessment of UHPC bridges

Tadesse G. Wakjira<sup>a,b</sup>, M. Shahria Alam<sup>a,\*</sup><sup>a</sup> School of Engineering, The University of British Columbia, Kelowna, BC, V1V 1V7, Canada<sup>b</sup> Idaho State University, 921 S 8th Ave, Pocatello, ID 83209, USA

## ARTICLE INFO

## Keywords:

Ultra-high-performance concrete (UHPC)  
 Fragility analysis  
 Resilience  
 Functionality  
 Machine Learning

## ABSTRACT

Efficient seismic vulnerability and resilience assessment is essential for ultra-high-performance concrete (UHPC) bridges, given their distinctive mechanical and structural properties. However, existing single-parameter-based probabilistic seismic demand (PSD) models overlook critical bridge-specific characteristics and uncertainties. Besides, studies on seismic vulnerability and resilience assessment of UHPC bridges are scarce. Thus, this study proposes a hybrid machine learning (ML)-enabled multivariate bridge-specific seismic vulnerability and resilience assessment framework for UHPC bridges. Key design parameters and associated uncertainties are identified, and a Latin Hypercube Sampling (LHS) technique is employed to establish a representative UHPC bridge database, which is used to develop a hybrid ML model-based multivariate PSD model. A comparative analysis with the conventional PSD model, as well as widely used ML algorithms, demonstrated that the proposed PSD model achieves the highest predictive performance, characterized by the highest coefficient of determination and lowest prediction errors. Additionally, SHapley Additive exPlanation (SHAP) analysis is used to investigate the effect of different parameters on the PSD of UHPC bridges. The results of SHAP show the peak ground acceleration (PGA) as the most important factor, followed by bridge span and column diameter. The hybrid ML-enabled multi-variate bridge-specific fragility analysis results are used to investigate the functionality recovery and resilience of the bridge, which demonstrate the reduction in the residual functionality and overall bridge resilience with the increase in the ground motion intensity.

## 1. Introduction

Despite its robust properties, bridges made with ultra-high-performance concrete (UHPC) are not exempt from the threats posed by earthquakes, which can lead to significant human and economic consequences. This reality highlights the importance of seismic vulnerability assessments in UHPC bridges. Such assessment plays a key role as it provides data for proactive risk reduction and prioritizes structural upgrades or retrofits [1,2]. A fundamental part of these assessments is seismic fragility analysis, which is a probabilistic approach that estimates the likelihood of a structure or its components meeting or exceeding a particular limit state during an earthquake of a specified intensity measure (IM) [3–5]. This approach ensures that bridges are constructed with advanced materials but are also designed to endure the challenges posed by natural disasters.

Numerous techniques, such as analytical, empirical, experimental, and hybrid techniques, have been introduced for seismic fragility assessment of civil infrastructures, with the analytical methods being the most frequently used approach [6–9]. However, these methods suffer from either poor resolution or the need for excessive time and computa-

tional resources [3]. The most widely used analytical fragility analysis approach, for instance, often necessitates substantial computational resources through nonlinear time history analysis (NLTHA) to compute the engineering damage parameters (EDPs) of concern, such as drift. In addition, the conventional approach for fragility analysis assumes that structures with similar configurations will suffer comparable damage levels under a given excitation. Consequently, fragility curves are typically established for specific types of bridges and structural systems based on a chosen classification system [10]. However, this method may undermine the reliability of loss assessment when applied to a diverse range of bridges that vary significantly within a particular class, as it does not consider vital bridge attributes, such as geometries. Additionally, classification criteria may be subjective or vary by region [10].

Moreover, developing a practical and effective framework for probabilistic seismic demand (PSD) models [11], which are integral to deriving analytical fragility curves, presents significant challenges [12]. Limitations of classical regression techniques in developing PSD models include fixed functional forms, inability to capture nonlinearity, and prior assumptions of lognormal distribution [13]. The inherent inflexibility of the conventional unidimensional PSD model makes it challenging to

\* Corresponding author.

E-mail address: [shahria.alam@ubc.ca](mailto:shahria.alam@ubc.ca) (M.S. Alam).

accommodate diverse sources of uncertainties, such as bridge geometrics and material characteristics, which could potentially undermine the reliability of the estimated demands [13]. Furthermore, the predefined distribution may not be suitable for all EDPs and bridge classes, as the distribution of demands is typically unknown in prior [12].

The emergence of advanced machine learning (ML) techniques driven by advances in computer technology provides an efficient alternative to conventional statistical procedures owing to their efficacy in managing complex data. ML techniques facilitate the development of more accurate fragility functions. As a result, various ML techniques have been explored to improve the fragility assessment of buildings [14,15] and conventional bridges [16–21]. For instance, Lagaros and Fragiadakis [22] and Mitropoulou and Papadrakakis [15] utilized ANN for the fragility assessment of steel frames and buildings, respectively. In addition, Mangalathu et al. [10] used ANN for the development of PSD models and fragility functions of conventional bridges. Pang et al. [17] and Mo et al. [19] utilized ANN and support vector machines, respectively, for the fragility assessment of conventional highway bridges. However, the full potential of ML models in enhancing the fragility assessment of bridges remains to be fully explored despite their widespread use in various fields. Moreover, a recent comprehensive review by Soleimani and Hajjalizadeh [12] underscores the limited extent of research conducted on the application of ML techniques for seismic fragility analysis of bridges. Furthermore, the scope of existing studies is generally limited as they typically concentrate on a limited set of input features and favor certain ML models without thoroughly investigating the potential of other ML models [12]. Besides, there is currently a lack of research on the bridge-specific multivariate seismic fragility assessment of UHPC bridges.

Therefore, this study introduces a novel framework for multivariate and bridge-specific seismic fragility and resilience assessment of UHPC bridges based on the hybrid ML model optimized with Optuna. Different parameters that characterize the uncertainties in geometry, material, and ground motion are considered. The efficacy of the hybrid ML model is then assessed against a conventional PSD model as well as a diverse spectrum of ML models of varying complexity levels. Furthermore, this research investigates the influence of these factors on the PSD for UHPC bridge columns using the SHAP approach [23].

## 2. Methodology

### 2.1. Hybrid ML model

Inspired by the error reduction strategy inherent in the boosting algorithm, the hybrid ML model is capable of providing an improved and stronger final model. The training procedure for the hybrid ML model begins with the establishment of a primary ensemble model. This model initially predicts the target variable using the selected primary ensemble model, with residuals calculated from the observed discrepancies between actual values and predictions. These residuals serve as the training foundation for secondary models. The type and number of the secondary models, as well as the hyperparameters of all the secondary and primary models, are tuned using Optuna, which is a state-of-the-art hyperparameter optimization algorithm. The working mechanism of the hybrid ML model is summarized below:

---

#### Algorithm 1 Hybrid ML Model for Enhanced Predictive Performance

---

- 1: **Given:**  $J$ : Total number of secondary models,  $M_j|_{j=1}^J$
  - 2: **Input:** Training dataset, primary ensemble model, and a pool of candidate secondary models ( $M_j|_{j=1}^J$ )
  - 3: **Initialize** the primary ensemble model:
  - 4: Compute the predictions of the primary ensemble model ( $\hat{Y}_{ens}^1$ )
  - 5: Compute the residuals:  $R_{ens}^1 = Y(i) - \hat{Y}_{ens}^1$ ,  $i = 1, 2, \dots, N$
  - 6: Set  $j = 1$ , where  $J$  represents the total number of secondary models required for improved predictive performance
  - 7: **for**  $j = 1$  to  $J$  **do**
  - 8:     **for**  $p = 1$  to  $P$  **do**
  - 9:         Sample  $m$  sets of secondary models from the candidate pool
  - 10:         Optimize hyperparameters and determine weights using  $R_{ens}^1$  with Optuna
  - 11:         Train the selected models with optimized hyperparameters
  - 12:         Compute the predictions of model  $j$ :  $\hat{Y}_j^1$
  - 13:         Evaluate predictive performance using RMSE
  - 14:         **if** predictive performance improves **then**
  - 15:             Update the hybrid model:
 
$$\hat{Y}_{hybrid}^1 = \hat{Y}_{ens}^1 + \sum_{d=1}^m \eta_d \hat{Y}_d^1, \quad \text{where } \eta_d = \frac{w_d}{\sum_{d=1}^m w_d}$$
  - 16:         Increment  $p$  by 1
  - 17:         **else**
  - 18:             Return to step (a) with a different model type and/or count from the candidate pool
  - 19:         **end if**
  - 20:     **end for**
  - 21: **end for**
  - 22: **Output:** Hybrid ML model with enhanced predictive performance
-

As outlined in the algorithm above, a key strength of the hybrid ML model is its adaptability in selecting optimal secondary models through an iterative process. The system employs advanced hyperparameter optimization, specifically Optuna, to identify the most effective model configurations. This ensures that each newly added model meaningfully contributes to reducing predictive error, thereby enhancing the overall predictive performance of the model. Additionally, the hybrid approach improves model robustness and generalizability by mitigating overfitting and effectively capturing complex data relationships. By integrating multiple models, the framework ensures a more reliable and scalable solution applicable to diverse datasets. Further details of the hybrid ML algorithm can be referred to elsewhere [24].

## 2.2. Seismic fragility

Seismic fragility defines the conditional probability of a structure exceeding a predetermined limit state when subjected to various ground motion intensity levels [25]. The fragility curve, in this context, represents the conditional probability of failure. Here, the term failure does not exclusively denote a complete structural collapse; rather, it implies a scenario in which the structural demand surpasses a predefined limit of capacity. Seismic fragility models employ this principle to calculate the conditional probability of exceeding a given damage state (DS) following an earthquake event of a specific intensity measure level ( $IM = \alpha$ ), as defined in Eq. (1):

$$P_f(\alpha) = P(DM > D_s | IM = \alpha) \quad (1)$$

A critical step in the fragility curve development of bridges involves implementing the PSD model to probabilistically compare the demands and capacities of different bridge components. This model estimates the likelihood of meeting or surpassing a specified demand level under a given intensity of ground motion. The conventional PSD model is based on a single parameter, namely, the ground motion intensity measure, as given in Eq. (2) [26], where  $S_D$  denotes the median value of the EDP:

$$\ln(S_D) = a + \ln(IM) \quad (2)$$

In this study, the drift ratio, which is the most widely used engineering damage parameter, is used as a key indicator of seismic demand of bridge column considering four distinct damage states; namely, slight (minimal damage), moderate (damage that can be repaired), extensive (extensive damage), and complete (probable replacement).

Fig. 1 summarizes the methodology adopted in this study to develop a novel hybrid ML-based framework for multivariate and bridge-specific fragility assessment of UHPC bridges. The proposed method involves the following steps:

- (a) **Generation of database:** This step involves the identification of important input parameters that influence the seismic vulnerability of UHPC bridges, the identification of the distribution of each parameter, and the generation of a database of  $M$  bridge samples using Latin hypercube sampling (LHS) technique. Each bridge sample is then paired with specific ground motion based on the site where the bridge is located to form  $M$  database of input parameters ( $X_M^K$ ), as given in Eq. (3), where  $K$  is the number of input parameters. In this study, the bridges are assumed to be located in Vancouver, British Columbia, Canada.

$$X_M^K = \begin{bmatrix} X_1^1 & X_2^1 & \dots & X_M^1 \\ X_1^2 & X_2^2 & \dots & X_M^2 \\ \vdots & \vdots & \ddots & \vdots \\ X_M^K & X_M^K & \dots & X_M^K \end{bmatrix} \quad (3)$$

In the next step, a 3D finite element model of highway bridges is developed for this purpose. An NLTHA is then conducted for each bridge sample to determine the seismic demand, which is used as a response variable in the next step. Furthermore, it is necessary to integrate the fragility functions with respect to the

**Table 1**

Drift ratio capacity uncertainty parameters for UHPC bridge piers [30].

Damage state	Parameters	
	$S_c$	$\beta_c$
DS1	1.93	0.27
DS2	3.14	0.26
DS3	5.04	0.33
DS4	6.19	0.36

ground motion IMs to determine the probability of exceedance at each damage state. In this study, peak ground acceleration (PGA) is adopted as the IM for demand modelling. This choice is supported by previous research, which has demonstrated the effectiveness of PGA in developing fragility curves for bridges [27–29].

- (b) **PSD model development using hybrid ML:** In this step, the input parameters are paired with each seismic demand to form a database for training different ML models, including hybrid ML model and other widely used ML models. The ML models are trained and tested on 80 % and 20 % of the complete dataset, respectively.
- (c) **Evaluation of the model:** The proposed model is then evaluated and compared against a wide range of ML models varying in their degree of complexity as well as the conventional single parameter-based PSD model.
- (d) **Fragility curve generation:** In this step, a new set of bridge samples ( $10^6$  in this study) are generated using LHS. The seismic demands of each sample are then determined using the optimized hybrid ML model. Once seismic demand estimates are obtained, fragility analysis necessitates capacity estimates that serve as thresholds at each limit state. The distribution and parameters of this distribution for the capacity of UHPC bridge columns, namely, the median estimate value for structural capacity ( $S_c$ ) and measure of dispersion around the median ( $\beta_c$ ) are obtained from a previous study by the authors [30], as listed in Table 1. The seismic demand is then compared with the structural capacity of the bridges to determine whether the corresponding damage states have been reached, and a value of 0 and 1 are assigned to represent the reached damage state or no, respectively. The fragility curve is then constructed using logistic regression based on the probability of failure at different intensity measures.
- (e) **Functionality recovery and resilience curves generation:** Based on the results of the fragility analysis, the functionality recovery and resilience curves are generated, as discussed in the following subsection. The application of the hybrid ML-based fragility model in this study enables the generation of multivariate and bridge-specific fragility curves at different damage states. The fragility curves derived from the methodology described above offer critical information for efficient seismic vulnerability assessment of UHPC bridges and enable informed decision-making in bridge design and retrofitting.

## 2.3. Seismic resilience

Fig. 2 shows the schematic representation of resilience. In seismic engineering, resilience is defined as the ability of a system to maintain or rapidly restore functionality after an earthquake. Functionality, in the context of a structure or infrastructure, can be described as its ability to provide adequate service to the users [31]. The functionality at time  $t$  (measured from the end of the occurrence of seismic event) under a given IM level is denoted  $Q(t/IM)$ , which can range from 0 (completely

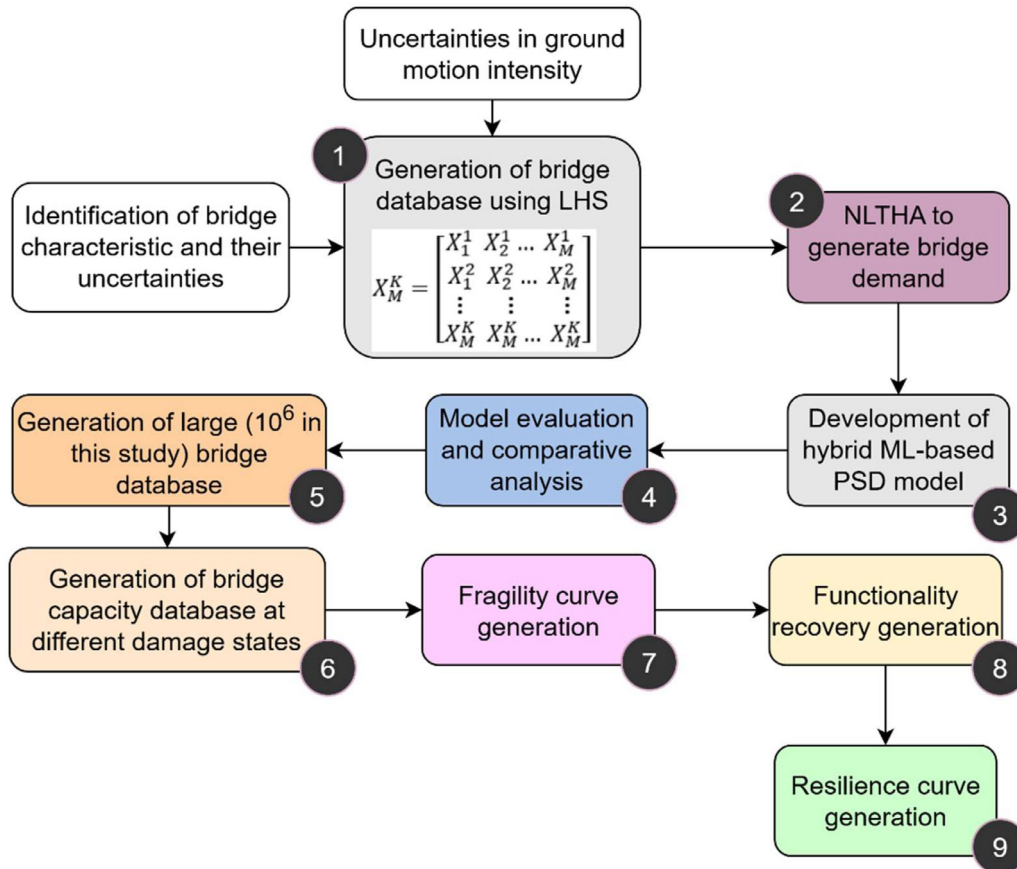


Fig. 1. Hybrid ML-enabled multivariate seismic vulnerability and resilience assessment of UHPC bridges.

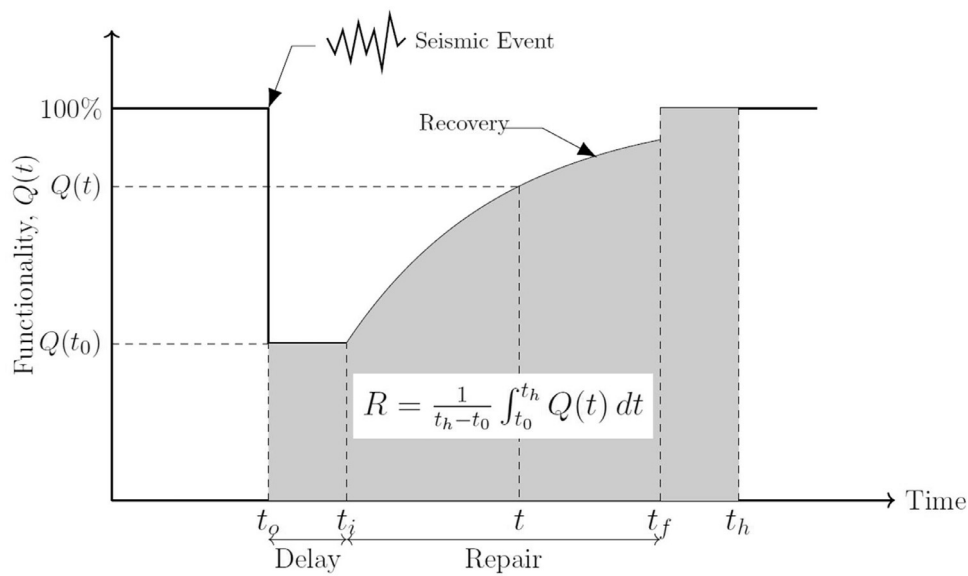


Fig. 2. Graphical representation of seismic resilience [31].

non-functional) to 1 (fully functional), as shown in Fig. 2.

$$Q(t/IM) = \sum_{k=0}^4 [Q^{(DS_k)}(t) (P^{(DS_k)}(IM) - P^{(DS_{k+1})}(IM))] \quad (4)$$

Where  $P^{(DS_k)}(IM)$  denotes the probability of being in the  $k^{\text{th}}$  damage state ( $DS_0$ : no damage,  $DS_1$ : slight damage,  $DS_2$ : moderate damage,  $DS_3$ : extensive damage, and  $DS_4$ : complete damage) and  $Q^{(DS_k)}(t)$  is

the functionality of the bridge for damage state  $DS_k$ , as given below:

$$Q^{(DS_k)}(t) = \begin{cases} Q_r, & \text{if } t < t_i \\ Q_r + H(\tau)R_f(\tau)(Q_i - Q_r), & \text{if } t_i < t < t_f \\ Q_i, & \text{if } t \geq t_f \end{cases} \quad (5)$$

where  $H(\cdot)$  is the Heaviside unit step function,  $Q_r$  is the residual functionality at the initial time  $t_i$  at which restoration starts (see Fig. 2),  $Q_i$

**Table 2**  
Distribution of parameters that describe the evolution of functionality over time across various damage states [31].

Parameter	Distribution		Damage state				
	Distribution type	Distribution parameters	No damage	Slight damage	Moderate damage	Extensive damage	Complete damage
Residual functionality, $Q_r$	Triangular	Minimum	1	0.5	0	0	0
		Maximum	1	1	0.5	0.2	0
		Mode	1	0.75	0.25	0.1	0
Idle time, $\varphi_i$ in months	Uniform	Minimum	–	1	1	1	1
		Maximum	–	2	2	2	2
Recovery duration, $\varphi_r$ in months	Triangular	Minimum	–	0.333	0.667	2	2.5
		Maximum	–	5	6.667	8.333	10
		Mode	–	2.667	3.667	5.167	6.25
Target functionality, $Q_t$	Triangular	Minimum	–	1	1	1	1
		Maximum	–	1	1	1	1
		Mode	–	1	1	1	1

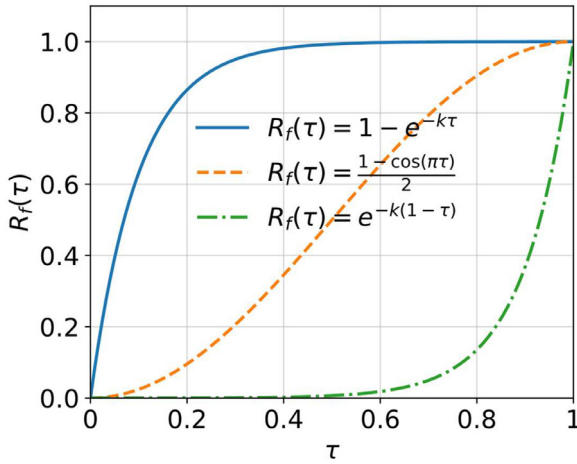


Fig. 3. Recovery functions.

is the target functionality at the end of the recovery time  $t_f$ ,  $t$  is the current time (after the earthquakes),  $\tau = (t - t_i)/(t_f - t_i)$ , and  $R_f(\cdot)$  is the recovery function.

After the idle time ( $\varphi_i = t_i - t_0$ ) ends where  $t_0$  is the time at which an earthquake occurs, the functionality of the structure ramps up from  $Q_r$  toward  $Q_t$ , as shown in Fig. 2. However, the shape of this recovery can vary depending on the damage severity. Thus, it is important to implement distinct recovery strategies [32]. In this study, three types of recovery functions; namely, negative-exponential recovery (often assigned to slight damage, DS1), sinusoidal recovery (often assigned to moderate damage, DS2), and positive-exponential recovery (often assigned to extensive, DS3, and complete damage, DS4) are used for different damage states, as given in Eqs. (6a)–(6c) and Fig. 3, respectively [31].

$$R_f(\tau) = 1 - e^{-k\tau} \tag{6a}$$

$$R_f(\tau) = \frac{1 - \cos(\pi\tau)}{2} \tag{6b}$$

$$R_f(\tau) = e^{-k(1-\tau)} \tag{6c}$$

where  $k$  is the shape parameter often set to 10 [32].

The residual functionality, idle time, recovery duration ( $\varphi_r = t_f - t_i$ ), and target functionality are random variables with the distribution given in Table 2. In this study, LHS is used to generate 100,000 combinations of these variables, and the mean functionality of the bridge over time at a given intensity measure is determined. The overall functionality of the bridge at a given intensity measure,  $Q(t|IM)$ , can then be determined by weighting the random samples with the fragility probabilities. Finally,

the resilience index at a given intensity measure  $R$  can be calculated as the area under the functionality curve (Fig. 2), as given below [31].

$$R(IM) = \frac{1}{t_h - t_0} \int_{t_0}^{t_h} Q(t|IM) dt \tag{7}$$

### 3. Case study

#### 3.1. Bridge description and ground motion characteristics

Concrete box girder bridges, which constitute the majority of the bridge inventory in British Columbia, Canada [33], were selected to demonstrate the proposed hybrid ML-based procedures in this study. As discussed earlier, the analysis considers multiple sources of uncertainty of bridge attributes, as presented in Table 3 [10,25,35], along with uncertainties in ground motion. The distribution and parameters of UHPC’s compressive strength were established based on the recently optimized sustainable UHPC [34]. For the remaining parameters, their distribution and the characteristics of their distribution were identified through a thorough literature review [10,25,35] with characteristics representative of those found in British Columbia, Canada. Highway bridge columns with an aspect ratio that ranges between 4 and 10, thus representing flexural dominated bridge piers [36], are considered in this study. The diameter of the bridge column ( $D_c$ ) is determined as a ratio of the pier height and aspect ratio. LHS is employed to generate 1520 statistically significant samples of bridges using the parameters’ distributions in Table 3. The LHS offers a method for efficient sampling from the variable distributions [37–41] and guarantees that each derived bridge class sample set accurately reflects the range of all parameters. Therefore, it is important to note that the developed model for this case study is most applicable and generalizable to bridge configurations within the parameter ranges specified in Table 3. However, its accuracy may be limited for bridge structures with significantly different characteristics, and further validation is recommended for applications beyond this range.

Twenty near-fault ground motion records from the PEER strong motion database [42] were selected for this study. The characteristics of the selected ground motion are presented in Table 4. These records feature original PGAs ranging from 0.11 to 0.85 g and are located within 10 km of the epicenter and, thus, are representative of near-field seismic effects [43]. The selected ground motions were spectrally matched to the uniform hazard design response spectra of Vancouver, British Columbia, Canada [30]. Additionally, the ground motion records are scaled with a scaling factor ranging from 0.25 to 4.0 at 0.05 increment, resulting in a total of 1520 varied ground motions. Each bridge sample was randomly associated with a distinct ground motion. Subsequently, a 3D model of the bridges was developed in OpenSees, and NLTHA was conducted on all the combinations of bridge samples. The maximum column drift demand was recorded at the end of shaking for each excitation.

**Table 3**  
Uncertainty of bridge characteristics considered in this study [10,25,35].

Input features	Distribution type	Distribution parameters*	
		$\mu/L$	$\sigma/U$
Span length, $S$ (m)	Normal	41.15	10.61
Column height, $H_c$ (m)	Lognormal	7.13	1.15
Compressive strength of UHPC, $f_{UHPC}$ (MPa)	Normal	181.95	27.43
Volume fraction of fibers, $V_f$ (%)	Uniform	1.0	3.0
Transverse reinforcement ratio, $\rho_t$ (%)	Uniform	0.4	1.3
Longitudinal reinforcement ratio, $\rho_l$ (%)	Uniform	1.0	3.0
Yield strength of reinforcement bars, $f_y$ (MPa)	Normal	475.7	37.9
Width of the deck, $w_d$ (m)	Normal	12.8	0.61
Deck mass multiplication factor, $m_f$	Uniform	0.9	1.1
Foundation translational stiffness ratio, $K_{fr}$ (%)	Uniform	0.5	1.5
Foundation rotational stiffness ratio, $K_{fr}$ (%)	Uniform	0.5	1.5
Damping ratio, $d_r$ (%)	Normal	4.5	1.25

\*  $\mu$ : Mean for normal distribution;  $\sigma$ : standard deviation for normal distribution;  $L$ : lower value for uniform distribution; and  $U$ : upper value for uniform distribution.

**Table 4**  
Characteristics of selected ground motions.

S.N.	Earthquake	Year	Station	Distance to fault (kN)	Magnitude	PGV (cm/s)	PGA (g)
1	Chi-Chi	1999	CHY101	9.9	7.6	65	0.34
2	Northridge	1994	Newhall-Fire Sta	9.4	6.7	7	0.11
3	Imperial Valley	1940	El Centro Array #9	6.1	7	30.9	0.28
4	Kobe, Japan	1995	KJMA	1	6.9	91.1	0.83
5	Coalinga	1983	Oil City	9.5	5.2	13.6	0.37
6	Northridge	1994	Sepulveda Hospital	8.4	6.7	77.7	0.75
7	Imperial Valley	1979	Westmorland Fire	9.8	6.5	12	0.11
8	Northridge	1994	Arleta-Nordhoff Fire	8.7	6.7	41.1	0.35
9	Landers	1992	Lucerne	2.2	7.3	133.4	0.73
10	Loma Prieta	1989	Corralitos	3.9	6.9	56	0.65
11	Chi-Chi	1999	TCU050	9.5	7.6	36.7	0.15
12	Imperial Valley	1979	El Centro Array #5	4	6.5	48.9	0.53
13	Chi-Chi	1999	TCU067	0.6	7.6	92.1	0.5
14	Northridge	1994	Sylmar-Converter	5.2	6.7	121	0.85
15	Loma Prieta	1989	LG-Lexington	5	6.9	85.7	0.44
16	Coalinga	1983	Pleasant Valley P. P	8.4	6.4	39.4	0.3
17	Kobe, Japan	1995	Takatori	1.5	6.9	120.7	0.62
18	Loma Prieta	1989	Saratoga-Valley Coll	9.3	6.9	42.1	0.26
19	Kobe, Japan	1995	Port Island	3.3	6.9	90.7	0.35
20	Chi-Chi	1999	CHY080	2.7	7.6	106.8	0.81

### 3.2. Modelling of seismic response

In the process of analytical fragility evaluation, fragility curves are established through the execution of numerical simulations, which generate a set of seismic demand data samples that are subsequently used for training PSD models. In this study, the 3D numerical model of the bridge was developed using OpenSees [44]. Fig. 4 shows the schematic representation of the numerical model. The bridge piers were modelled using displacement-based beam-column elements. Each fiber section was divided into concrete fibers (cover and core fibers) and steel fibers. The longitudinal reinforcement is modelled using the uniaxial *Steel02* model in OpenSEES. The uniaxial stress-strain response of both unconfined and confined concrete was simulated using the OpenSees *Concrete01* material model. Thus, the tensile capacity of the concrete is not considered due to the lack of a reliable model to determine the tension response of UHPC. For the confined concrete, its properties at the peak and ultimate states were determined based on the stress-strain constitutive model developed in a previous study for confined UHPC with normal and high-strength spirals [45]. Additionally, the geometric nonlinearity is accounted for by incorporating the P-delta effect into the bridge columns. For dynamic analyses, Rayleigh damping is utilized to account for the first and second vibration modes.

Furthermore, bridge decks are modelled using elastic beam-column elements to reflect the expectation that they remain elastic during seismic events. Consequently, the effective stiffness of prestressed concrete

decks is represented by their gross stiffness without accounting for potential concrete cracking. Both diaphragms and expansion joints in the decks, as depicted in transverse deck elements (see Fig. 4), are simulated using elastic beam-column elements. These elements are designed to be rigid and massless. The deck elements are connected to the columns using rigid elements to facilitate the transfer of moments and forces between adjacent components. As shown in Fig. 4, expansion joints between the deck and abutment comprised elements such as elastomeric bearings (transverse and longitudinal), a transverse shear key, and a component to simulate pounding between the deck and abutment. Elastomeric bearings in the expansion joints are modelled as elastic-perfectly plastic elements. Pounding between the deck and abutment is represented using zero-length elements following Muthukumar and DesRoches [46] compression-only bilinear material model with a gap. The transverse shear key is simulated with a symmetric trilinear behaviour and a gap. Bridge foundations are modelled using lumped linear translational and rotational springs with zero-length elements assigned at the center of the footings, as shown in Fig. 4.

### 3.3. Results and discussion

Different single and ensemble models such as k-nearest neighbor (KNN), support vector regression (SVR), gradient boosting machine (GBM), and extreme gradient boosting (XGB) are investigated for use as the base learner for the hybrid ML model. Based on the results of prelimi-

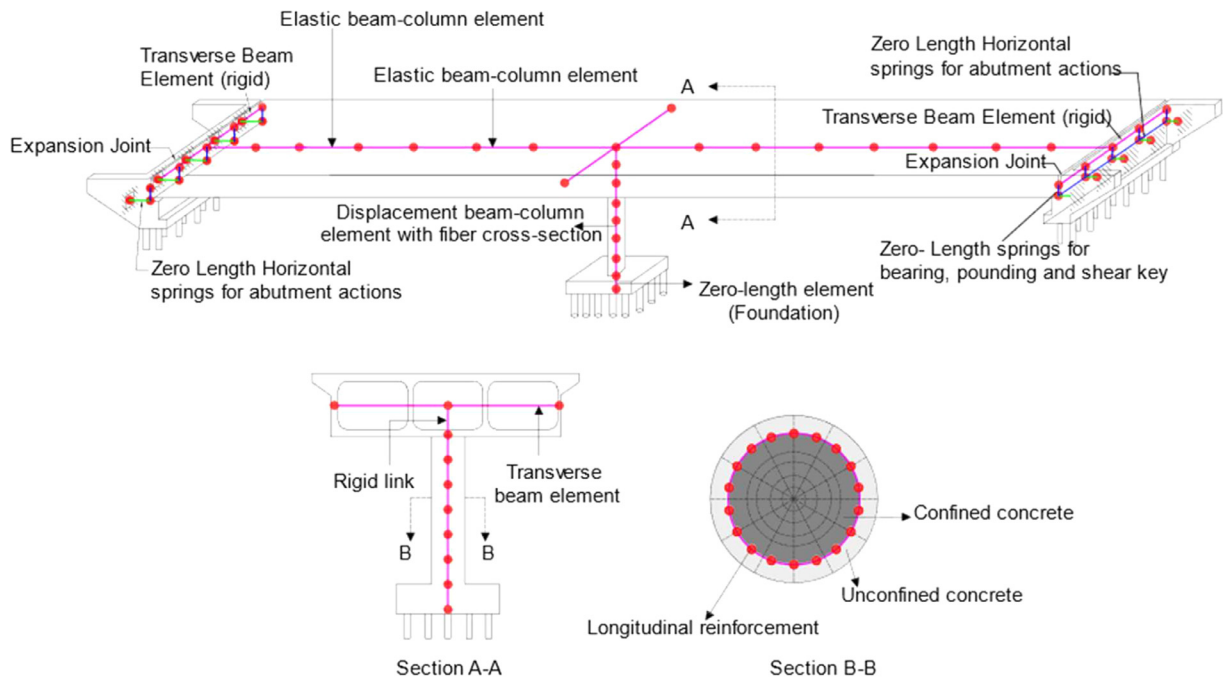


Fig. 4. Numerical model of the selected bridge.

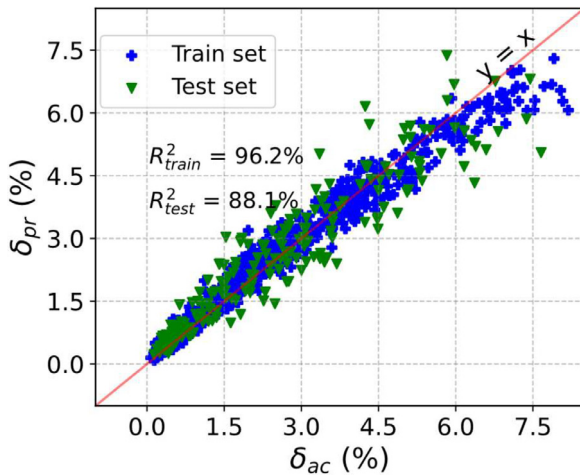


Fig. 5. PSD of UHPC column drift demand.

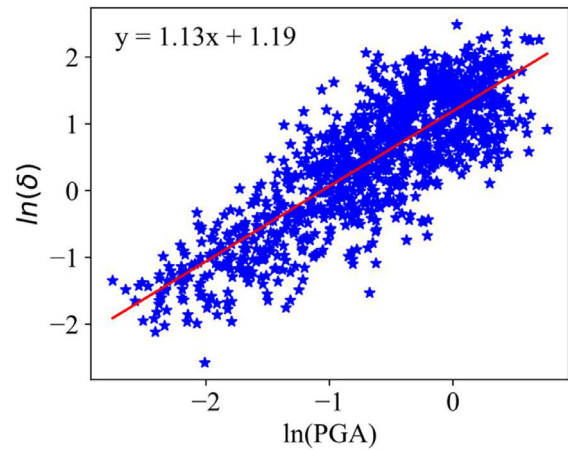


Fig. 6. PSD for column drift based on conventional method.

nary investigations, XGB is used as the primary model, while GBM, KNN, and SVR are used as the secondary models in the proposed hybrid ML model. The hyperparameters of both the primary and secondary models, as well as the weight of each secondary model, are optimized with the use of Optuna [47] in conjunction with 10-fold cross-validation. The training of the hybrid ML model was performed on a Razer laptop with an Intel Core i9 processor and 32GB RAM and required 1 hour and 57 min. Once trained, the inference phase remained highly efficient, with each sample processed in 4.2 milliseconds. The integration of Optuna for hyperparameter optimization further improved computational efficiency by automating the tuning process, reducing manual effort, and ensuring optimal model performance.

Fig. 5 shows the predicted versus actual PSD for the column drift ratio. Moreover, Table 5 presents the predictive performance of the model in terms of the different statistical performance metrics. As can be observed in Fig. 5, the hybrid ML model achieved a satisfactory level of prediction accuracy across both training and test datasets. Notably, the model demonstrated a strong ability to generalize to unseen data, as ev-

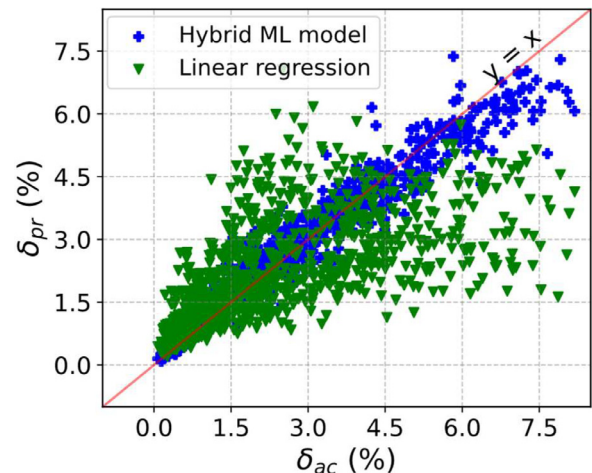


Fig. 7. Predicted versus actual PSD for column drift based on the conventional linear regression and proposed hybrid ML model.

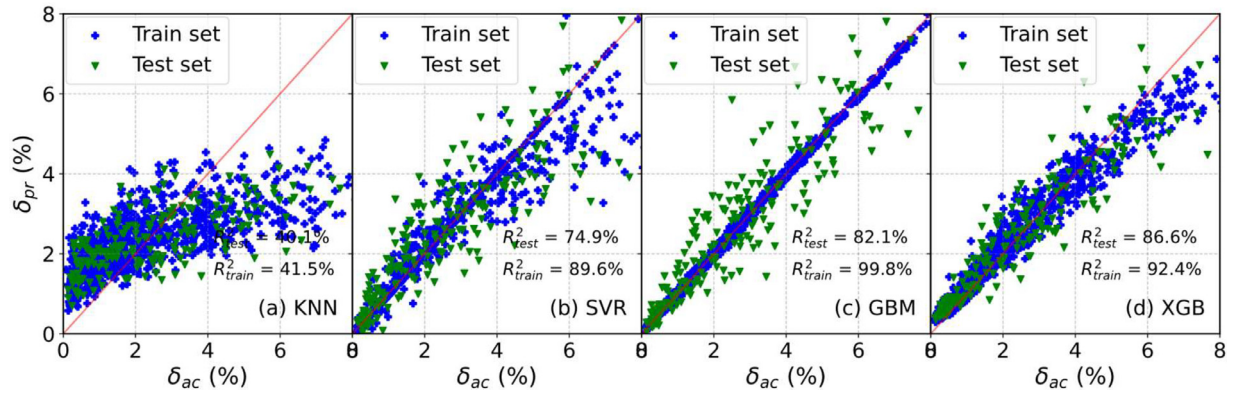


Fig. 8. PSD of UHPC column drift ratio based on different ML models.

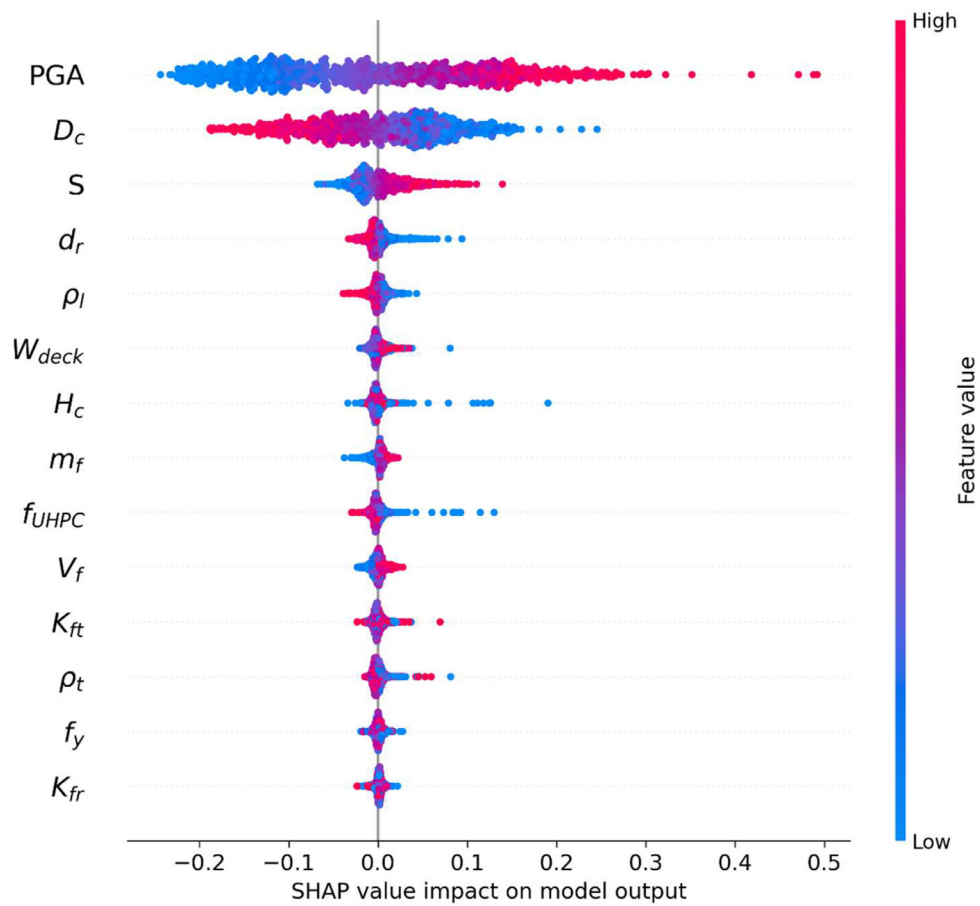


Fig. 9. SHAP summary plot.

**Table 5**  
Performance measures of PSD prediction for UHPC bridge columns' drift demand.

Model	Training dataset			Test dataset		
	RMSE (%)	MAE (%)	R <sup>2</sup> (%)	RMSE (%)	MAE (%)	R <sup>2</sup> (%)
KNN	1.54	1.15	41.46	1.44	1.18	40.05
SVR	0.65	0.29	89.64	0.93	0.68	74.86
GBM	0.09	0.07	99.81	0.79	0.56	82.12
XGB	0.55	0.35	92.44	0.68	0.49	86.65
Hybrid	0.39	0.25	96.17	0.64	0.47	88.10

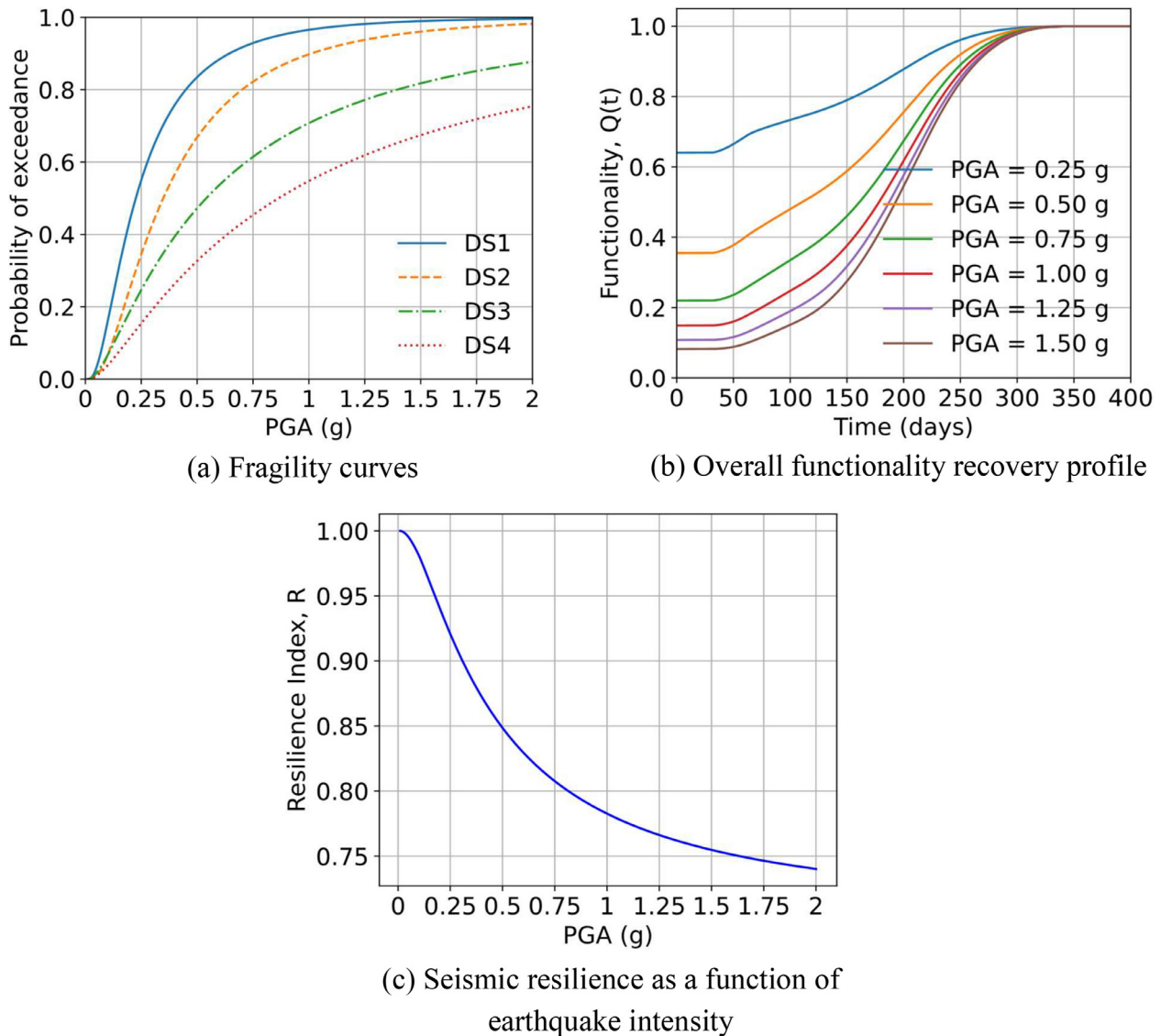


Fig. 10. Fragility curves generated based on the hybrid ML model and the resulting functionality recovery profile and seismic resilience.

indexed by the consistency of performance metrics between the training and testing phases. For instance, it achieved a remarkably low RMSE of 0.39 % in the training dataset and 0.64 % in the test dataset, which signifies a minimal deviation from the actual values, as listed in Table 5. Furthermore, the achieved MAE values of 0.25 % for training and 0.47 % for test datasets reinforce the prediction accuracy of the model, which highlights its consistent performance across different data sets (Table 5). Moreover, it showed a high coefficient of determination for both training and test datasets, as can be seen in Fig. 5 and Table 5.

Based on the conventional linear regression of the PSD model, the resulting equation is shown in Fig. 6. This figure also shows the resulting equation in which  $y = \ln(\delta)$  and  $x = \ln(IM)$ . Moreover, Fig. 7 compares the traditional PSD model with the proposed hybrid ML model in terms of the scatter plots of the predicted versus actual PSD for column drift demand. As can be seen in this figure, the conventional single variable (i.e., IM) based PSD model is inadequate, while the proposed hybrid ML-based multivariable PSD model showed a higher degree of predictive performance.

The accuracy of the proposed hybrid ML model is further investigated by comparing it to other ML models; namely, KNN, SVR, GBM, and XGB. It is observed that the proposed hybrid ML model has the highest PSD predictive performance with the lowest error metrics and highest

$R^2$  in comparison to other ML models, as listed in Table 5. Among the base models, the XGB model showed the highest prediction accuracy, while the KNN model showed the least prediction accuracy, as can be observed in Table 5. This can further be observed in Fig. 8, which compares the predicted versus actual values of the PSD result for column drift demand. As can be seen in this figure, the GBM showed a clear overfitting, while the other models showed poor performance across both the training and test datasets. However, the proposed hybrid ML model has superior prediction capability and generalization ability across unseen data as it leverages the strengths of individual models while mitigating their weaknesses in order to produce enhanced overall performance.

The SHAP method is used in this study to investigate the influence of different input features on the PSD for column drift ratio. Fig. 9 shows a SHAP summary plot in which the input factors are arranged on the y-axis by their level of impact on the PSD prediction, with the most influential factor at the top. Moreover, the magnitude of the influence of each input is presented in the x-axis through the SHAP values. As can be seen in Fig. 9, the ground motion intensity has the highest significant influence on the PSD for column drift. This result is in agreement with the previous study for conventional concrete bridges [10]. The bridge pier column diameter is found to be the second most influential parameter, followed by the span length and damping ratio. In addition to the order

of the significant effect of the input features, the SHAP summary plot shows the direction of their effect on the predicted PSD. For example, an increase in PGA and bridge span increased the drift demand, whereas a larger column diameter reduced the drift demand. In addition, the input features such as the damping ratio, concrete compressive strength, and longitudinal reinforcement ratio are shown to have a mitigating effect on drift demand, with their increase leading to reduced predicted drift demand.

Given its high predictive capability, the developed hybrid ML model is utilized to develop the fragility curves based on the methodology discussed earlier. The resulting fragility curves for the bridge column are shown in Fig. 10a for all four damage states. The developed multivariate fragility curves can then be used to determine the vulnerability of UHPC bridges and potential losses resulting from earthquakes. Using the fragility analysis results and the methodology presented in Section 2.2, the functionality and resilience of the bridge are evaluated. Fig. 10b illustrates the functionality recovery profiles of the bridge system under varying earthquake intensities. It can be observed that as the earthquake intensity increases, the residual functionality of the bridge system decreases due to the higher damage levels sustained. The recovery process is gradual, with functionality being restored over time; however, for higher PGA, the damage requires more extensive repair time. Fig. 10c shows the variation in the seismic resilience of the bridge as a function of earthquake intensity. A clear declining trend in resilience is observed with increasing PGA, which highlights the escalating challenges in restoring functionality. This trend reflects the compounded effects of higher damage levels, which not only prolong the repair process but also diminish the system's capacity to recover efficiently. As shown in this figure, the resilience of the bridge decreases with an increase in the ground motion intensity, which demonstrates more significant challenges in restoring functionality due to higher damage levels that prolong repairs and reduce recovery efficiency.

#### 4. Conclusions

An efficient seismic fragility assessment approach is essential to enable accurate seismic vulnerability assessment of UHPC bridges. However, the conventional seismic fragility assessment approach may not accurately reflect the varied nature of bridges within a specific category as it disregards critical bridge characteristics like bridge geometries. Moreover, there is a lack of seismic fragility and resilience assessment for UHPC bridges. Therefore, this study introduces a multivariate and bridge-specific seismic vulnerability and resilience assessment method for UHPC bridges. This method incorporates a hybrid ML model that accounts for uncertainties in bridge characteristics and ground motion. The proposed methodology involves a systematic identification and selection of the critical design parameters and their uncertainties, generation of the UHPC bridge database using the LHS technique considering different sources of uncertainties, determination of demand parameters at different damage states, generation of PSD models using hybrid ML model, generation of capacity and demand database using the proposed PSD models and uncertainty in the capacity, and generation of fragility curves. The effectiveness of the proposed approach is benchmarked against the conventional single parameter-based PSD model. Furthermore, the predictive performance of the proposed hybrid ML model is evaluated in comparison with widely used ML models in existing literature. Additionally, the SHAP method is employed to explore the impact of various factors on the PSD for the drift demand of the bridge column. The results of fragility analysis are used to perform functionality recovery and resilience assessment of the UHPC bridge.

The following conclusions can be drawn from the results of the current study:

- Among the models investigated for use as base learner for the hybrid ML model, the XGB emerged as the most effective model in predicting the PSD for column drift demand.

- The hybrid ML model achieved satisfactory accuracy in estimating the PSD for column drift ratios with a high coefficient of determination ( $R^2 = 88.1\%$ ) and low error metrics on the test set.
- Compared to traditional single parameter-based PSD models, the hybrid ML model exhibited significantly higher prediction accuracy. The conventional PSD model showed inadequate prediction accuracy. These results highlight the limitations of single parameter conventional PSD models in capturing drift demand complexities.
- The results of the SHAP analysis on the box-girder bridge used as a case study revealed that the ground motion intensity measure (PGA in this study) was the most influential factor on PSD for UHPC column drift demand, followed by the bridge span and column diameter.
- The proposed hybrid ML-based seismic vulnerability and resilience approach enables efficient and bridge specific seismic vulnerability and resilience assessment of UHPC bridges.
- The residual functionality of the bridge system decreases with an increase in the ground motion intensity due to the higher damage levels sustained. Consequently, higher intensities also lead to lower overall resilience of the bridge.

The developed multi-variate fragility assessment approach facilitates seismic vulnerability assessment and resilience assessment of UHPC bridges, thus supporting informed decision-making in bridge design and retrofitting. While this study presents a novel hybrid ML-based framework for evaluating UHPC bridges, its applicability is demonstrated using a case study focused on box-girder bridges. Nevertheless, additional research is necessary to explore the applicability of the proposed method across a broader range of UHPC bridge types beyond the box-girder bridges examined in this study. Furthermore, future studies could investigate the impact of training dataset size on model performance as well as evaluate the sensitivity of the model to different IMs to assess their influence on predictive accuracy and efficiency.

#### Relevance to resilience Content

The paper presents a hybrid machine learning-enabled framework for multivariate bridge-specific seismic vulnerability and resilience assessment of ultra-highperformance concrete (UHPC) bridges. It considers bridge-specific characteristics and uncertainties, which enables more accurate seismic demand modeling and fragility analysis. Thus, the study enhances proactive planning, informed decision-making, and adaptive responses to ensure the continued functionality and safety of UHPC bridges.

#### Declaration of competing interest

The authors declare that they have no known competing financial interests or personal relationships that could have appeared to influence the work reported in this paper.

#### CRedit authorship contribution statement

**Tadesse G. Wakjira:** Writing – review & editing, Writing – original draft, Visualization, Validation, Software, Methodology, Investigation, Formal analysis, Data curation, Conceptualization. **M. Shahria Alam:** Writing – review & editing, Validation, Supervision, Resources, Project administration, Methodology, Funding acquisition, Conceptualization.

#### Acknowledgment

The financial contribution of Kon Kast Concrete Products Inc and Mitacs through the Accelerate grant is gratefully acknowledged.

## References

- [1] Padgett JE, Desroches R, Nilsson E. Regional seismic risk assessment of bridge network in Charleston, South Carolina. *J Earthq Eng* 2010;14:918–33. doi:10.1080/13632460903447766.
- [2] Padgett JE, DesRoches R. Retrofitted bridge fragility analysis for typical classes of multispan bridges. *Earthq Spectra* 2009;25:117–41. doi:10.1193/1.3049405.
- [3] Choi E, DesRoches R, Nielson B. Seismic fragility of typical bridges in moderate seismic zones. *Eng Struct* 2004;26:187–99. doi:10.1016/j.engstruct.2003.09.006.
- [4] Nielson BG, Desroches R. Seismic fragility methodology for highway bridges using a component level approach. *Earthq Eng Struct Dyn* 2007;36:823–39. doi:10.1002/eqe.
- [5] Salkhordeh M, Govahi E, Mirtaheeri M. Seismic fragility evaluation of various mitigation strategies proposed for bridge piers. *Structures* 2021;33:1892–905. doi:10.1016/j.istruc.2021.05.041.
- [6] M S, MQ F, J L, T N. Statistical analysis of fragility curves. *J Eng Mech* 2000;126:1224–31.
- [7] P G, A DK, KM M. Probabilistic capacity models and fragility estimates for reinforced concrete columns based on experimental observations. *J Eng Mech* 2002;128:1024–38.
- [8] Rossetto T, Elnashai A. Derivation of vulnerability functions for European-type RC structures based on observational data. *Eng Struct* 2003;25:1241–63. doi:10.1016/S0141-0296(03)00060-9.
- [9] Billah AHMM, Alam MS. Seismic fragility assessment of highway bridges: a state-of-the-art review. *Struct Infrastruct Eng* 2015;11:804–32.
- [10] Mangalathu S, Heo G, Jeon JS. Artificial neural network based multi-dimensional fragility development of skewed concrete bridge classes. *Eng Struct* 2018;162:166–76. doi:10.1016/j.engstruct.2018.01.053.
- [11] Ang A-S, De Leon D. Modeling and analysis of uncertainties for risk-informed decisions in infrastructures engineering. *Struct Infrastruct Eng* 2005;1:19–31. doi:10.1080/15732470412331289350.
- [12] Soleimani F, Hajjalizadeh D. State-of-the-art review on probabilistic seismic demand models of bridges: machine-learning application. *Infrastructures (Basel)* 2022;7. doi:10.3390/infrastructures7050064.
- [13] Soleimani F. Probabilistic seismic analysis of bridges through machine learning approaches. *Structures* 2022;38:157–67. doi:10.1016/j.istruc.2022.02.006.
- [14] Kiani J, Camp C, Pezeshk S. On the application of machine learning techniques to derive seismic fragility curves. *Comput Struct* 2019;218:108–22. doi:10.1016/j.compstruc.2019.03.004.
- [15] Mitropoulou CC, Papadrakakis M. Developing fragility curves based on neural network IDA predictions. *Eng Struct* 2011;33:3409–21. doi:10.1016/j.engstruct.2011.07.005.
- [16] Kameshwar S, Padgett JE. Response and fragility assessment of bridge columns subjected to barge-bridge collision and scour. *Eng Struct* 2018;168:308–19. doi:10.1016/j.engstruct.2018.04.082.
- [17] Pang Y, Dang X, Yuan W. An artificial neural network based method for seismic fragility analysis of highway bridges. *Adv Struct Eng* 2014;17:413–28. doi:10.1260/1369-4332.17.3.413.
- [18] Wang M, Zhang H, Dai H, Shen L. A deep learning-aided seismic fragility analysis method for bridges. *Structures* 2022;40:1056–64. doi:10.1016/j.istruc.2022.04.058.
- [19] MO R, Chen L, Xing Z, Ye X, Xiong C, Liu C, et al. Bridge seismic fragility model based on support vector machine and relevance vector machine. *Structures* 2023;52:768–78. doi:10.1016/j.istruc.2023.03.179.
- [20] Xie Y, Ebad Sichani M, Padgett JE, DesRoches R. The promise of implementing machine learning in earthquake engineering: a state-of-the-art review. *Earthq Spectra* 2020;36:1769–801. doi:10.1177/8755293020919419.
- [21] Huang C, Huang S. Predicting capacity model and seismic fragility estimation for RC bridge based on artificial neural network. *Structures* 2020;27:1930–9. doi:10.1016/j.istruc.2020.07.063.
- [22] Lagaros ND, Fragiadakis M. Fragility assessment of steel frames using neural networks. *Earthq Spectra* 2007;23:735–52. doi:10.1193/1.2798241.
- [23] Lundberg S.M., Lee S.A. Unified Approach to Interpreting Model Predictions. 31st Conf. neural Inf. Process. Syst. (NIPS 2017), Long Beach, CA, USA: 2017, p. 1–10.
- [24] Wakjira TG, Alam MS. Peak and ultimate stress-strain model of confined ultra-high-performance concrete (UHPC) using hybrid machine learning model with conditional tabular generative adversarial network. *Appl Soft Comput* 2024;154. doi:10.1016/j.asoc.2024.111353.
- [25] Tavares DH, Padgett JE, Paultre P. Fragility curves of typical as-built highway bridges in eastern Canada. *Eng Struct* 2012;40:107–18. doi:10.1016/j.engstruct.2012.02.019.
- [26] Cornell CA, Jalayer F, Hamburger RO, Foutch DA. Probabilistic basis for 2000 SAC federal emergency management agency steel moment frame guidelines. *J Struct Eng* 2002;128:526–33.
- [27] Padgett JE, Nielson BG, Desroches R. Selection of optimal intensity measures in probabilistic seismic demand models of highway bridge portfolios. *Earthq Eng Struct Dyn* 2008;37:711–25. doi:10.1002/eqe.
- [28] Padgett JE, Desroches R. Methodology for the development of analytical fragility curves for retrofitted bridges. *Earthq Eng Struct Dyn* 2008;37:1157–74. doi:10.1002/eqe.
- [29] Mackie KR, Stojadinović B. Fragility basis for California highway overpass bridge seismic decision making Pacific earthquake engineering research center. Berkeley, USA: College of Engineering, University of California; 2005.
- [30] Wakjira TG, Alam MS. Performance-based seismic design of Ultra-High-Performance Concrete (UHPC) bridge columns with design example – Powered by explainable machine learning model. *Eng Struct* 2024;314. doi:10.1016/j.engstruct.2024.118346.
- [31] Decò A, Bocchini P, Frangopol DM. A probabilistic approach for the prediction of seismic resilience of bridges. *Earthq Eng Struct Dyn* 2013;42:1469–87. doi:10.1002/eqe.2282.
- [32] Pang Y, Wang X. Enhanced endurance-time-method (EETM) for efficient seismic fragility, risk and resilience assessment of structures. *Soil Dyn Earthq Eng* 2021;147. doi:10.1016/j.soildyn.2021.106731.
- [33] Siddiquee K, Shahria Alam M. Highway bridge infrastructure in the province of British Columbia (BC), Canada. *Infrastructures (Basel)* 2017;2. doi:10.3390/infrastructures2020007.
- [34] Wakjira TG, Kutty AA, Alam MS. A novel framework for developing environmentally sustainable and cost-effective ultra-high-performance concrete (UHPC) using advanced machine learning and multi-objective optimization techniques. *Constr Build Mater* 2024;416. doi:10.1016/j.conbuildmat.2024.135114.
- [35] Nielson B.G. Analytical fragility curves for highway bridges in moderate seismic zones. 2005. <https://doi.org/10.1016/j.istruc.2017.03.041>.
- [36] Zhu L, Elwood KJ, Haukaas T. Classification and seismic safety evaluation of existing reinforced concrete columns. *J Struct Eng* 2007;133:1316–30. doi:10.1061/(ASCE)0733-9445(2007)133:9(1316).
- [37] McKay MD, Beckman RJ, Conover WJ. A comparison of three methods for selecting values of input variables in the analysis of output from a computer code. *Technometrics* 1979;21:239–45.
- [38] Olsson A, Sandberg G, Dahlblom O. On Latin hypercube sampling for structural reliability analysis. *Struct Saf* 2003;25:47–68.
- [39] Wei B, Zheng X, Jiang L, Lai Z, Zhang R, Chen J, et al. Seismic response prediction and fragility assessment of high-speed railway bridges using machine learning technology. *Structures* 2024;66. doi:10.1016/j.istruc.2024.106845.
- [40] Zaker Esteghamati M, Flint MM. Developing data-driven surrogate models for holistic performance-based assessment of mid-rise RC frame buildings at early design. *Eng Struct* 2021;245. doi:10.1016/j.engstruct.2021.112971.
- [41] Ding JY, Feng DC, Brunesi E, Parisi F, Wu G. Efficient seismic fragility analysis method utilizing ground motion clustering and probabilistic machine learning. *Eng Struct* 2023;294. doi:10.1016/j.engstruct.2023.116739.
- [42] PEER Pacific earthquake engineering research center, strong motion database Available from <http://ngawest2.berkeley.edu/>.
- [43] CSA. Csa S6-14Canadian highway bridge design code. Mississauga: Can Stand Assoc (CSA); 2014.
- [44] Mckenna F. OpenSees: a framework for earthquake engineering simulation. *Comput Sci Eng* 2011;13:58–66.
- [45] Wakjira TG, Abushanab A, Alam MS. Hybrid machine learning model and predictive equations for compressive stress-strain constitutive modelling of confined ultra-high-performance concrete (UHPC) with normal-strength steel and high-strength steel spirals. *Eng Struct* 2024;304. doi:10.1016/j.engstruct.2024.117633.
- [46] Muthukumar S, DesRoches R. A Hertz contact model with nonlinear damping for pounding simulation. *Earthq Eng Struct Dyn* 2006;35:811–28. doi:10.1002/eqe.557.
- [47] Akiba T, Sano S, Yanase T, Ohta T, Koyama M. Optuna: a next-generation hyperparameter optimization framework. *Proc ACM SIGKDD Int Conf Knowl Discov Data Min* 2019:2623–31. doi:10.1145/3292500.3330701.